Lithium-Ion Batteries

DOI: 10.1002/anie.200701628

Formation of Lithium-Driven Active/Inactive Nanocomposite Electrodes Based on $Ca_3Co_4O_9$ Nanoplates

Dong-Wan Kim, Young-Dae Ko, Jae-Gwan Park, and Byung-Kook Kim*

The increasing demand for portable power has generated significant interest in studying high-performance lithium-ion batteries.[1,2] To date, graphite has been used as the anode material in this type of batteries, but its limited theoretical gravimetric capacity (of 372 mA h g^{-1}) has inspired intensive research toward alternative anode materials.[3–5] In particular, transition-metal oxides (that is, *M*O, where *M* is Co, Ni, Cu or Fe) have been reported to exhibit an extremely large reversible capacity, which arises from their displacement reactions.[6] However, the practical use of metal oxides, such as Co_3O_4, has been limited by their fast capacity fading and their poor cycle-life performance.[7,8] Part of the problem associated with these materials may be attributed to the significant volume changes that occur during lithium uptake and removal (the molar volume changes about 100%), which may result in a loss of electrical contact and in electrode failure.[9] In addition to designing *M*O–carbon composites to prevent the aggregation of the particles and the resultant loss of electrical contact, the formation of active/inactive composites has also gained attention for obtaining an improved cycling performance in ternary metal-oxide systems.[9–11]

Ternary metal oxides are also being actively investigated as thermoelectric materials for use in energy-harvesting systems because of their high thermal stability, oxidation resistance, and reduced toxicity.[12,13] Layered cobaltite (that is, $Ca_3Co_4O_9$) has received special attention. This compound, which has a misfit structure consisting of a single CdI_2-type [CoO_2] layer stacked with [$CoCa_2O_3$] rock-salt-type layers with different in-plane lattice parameters *b*, has been reported to have high thermoelectric properties.[14–16]

Herein, we report the first application of a thermoelectric material, namely, $Ca_3Co_4O_9$ nanoplates with high electrical conductivity, to a Li-ion-battery anode. Furthermore, the formation of lithium-active/inactive nanocomposites during the charge/discharge process is carefully investigated.

Figure 1a shows an X-ray diffraction (XRD) pattern of the calcined powder prepared by using the citrate-gel method. This powder can be indexed as a misfit-layered oxide consisting of two monoclinic subsystems, thus demonstrating the presence of crystalline $Ca_3Co_4O_9$.[12] It can be clearly seen in Figure 1b,c that the powders obtained by means of calcination at 600 °C (for 12 h) are composed of very thin, micalike nanoplatelets with average lateral sizes below 50 nm. The powders calcined at 700 °C for 2 h have a similar two-dimensional morphology, with an increased thickness of the order of 10–50 nm and an average lateral size of around 300 nm (see Figure S1 of the Supporting Information). The [100] image taken along the cross-section of the nanoplates in the powder calcined at 700 °C for 2 h is in good agreement with the calculated image. A variation in the contrast—observed in Figure 1d—is attributed to the layered structure

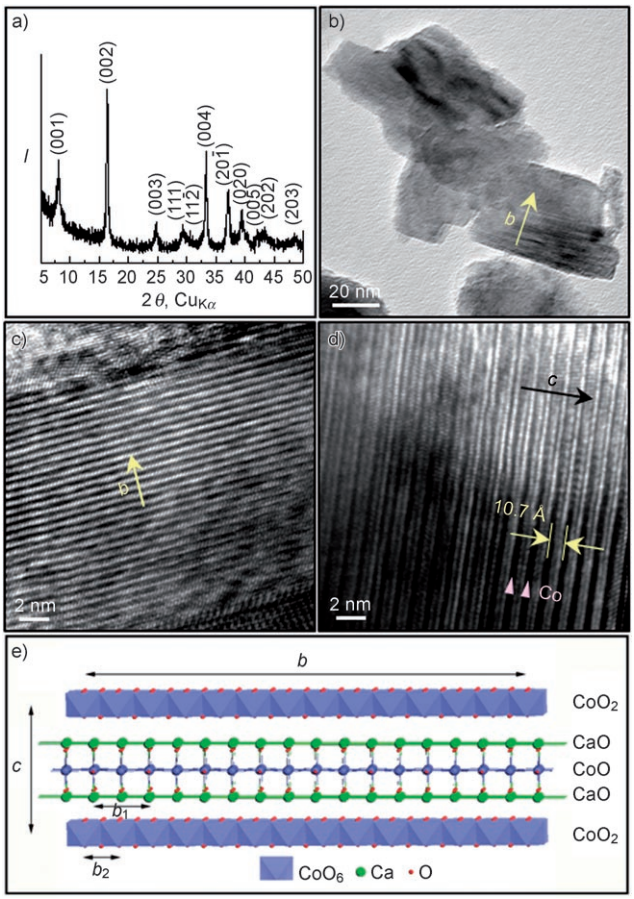

Figure 1. a) XRD pattern, b) TEM image, and c) [001] high-resolution transmission electron microscopy (HRTEM) image of the nanosized $Ca_3Co_4O_9$ powders calcined at 600 °C for 12 h in O_2. d) [100] HRTEM image along the cross-section of a $Ca_3Co_4O_9$ nanoplate calcined at 700 °C for 2 h in O_2. e) Proposed structural model for $Ca_3Co_4O_9$ involving a supercell with $b \approx 8b_1 \approx 13b_2$.

[*] Dr. D.-W. Kim, Y.-D. Ko, Dr. J.-G. Park
Nanoscience Research Division
Korea Institute of Science and Technology
Seoul 136-791 (South Korea)
Fax: (+82) 2-958-5489
E-mail: dwkim@kist.re.kr
Dr. B.-K. Kim
Materials Science and Technology Division
Korea Institute of Science and Technology
Seoul 136-791 (South Korea)

Supporting information for this article is available on the WWW under http://www.angewandte.org or from the author.

WILEY InterScience DISCOVER SOMETHING GREAT
© 2007 Wiley-VCH Verlag GmbH & Co. KGaA, Weinheim

of $Ca_3Co_4O_9$, which is built up from the stacking along the *c* axis of alternating triple rock-salt-type layers of $[CaO–CoO–CaO]_\infty$ with single CdI_2-type layers of $[CoO_2]_\infty$ (marked by arrows in Figure 1 d)).[16]

The $[CoO_2]_\infty$ layers are spaced by a distance of 10.7 Å, which is consistent with the lattice parameter *c* of $Ca_3Co_4O_9$. Figure 1 e shows a schematic representation of the crystal structure of $Ca_3Co_4O_9$ involving the proposed stacking mode of the layers.[15,16] This layered structure could be closely related to the behavior of the electrons in an anisotropic structural environment, which results in high electrical conductivity. Indeed, the electrical conductivity of the sintered samples of $Ca_3Co_4O_9$ (namely, 34 $S\,cm^{-1}$) is much higher than that of the normal spinel-type Co_3O_4 samples (that is, 1.96×10^{-5} $S\,cm^{-1}$), which was measured by using a conventional two-probe direct-current (dc) technique at room temperature.[17,18] This unusually high electrical conductivity of $Ca_3Co_4O_9$ would make it useful for the reaction kinetics, especially during the first-lithiation process.

We evaluated the electrochemical activity of $Ca_3Co_4O_9$ by means of cyclic voltammetry (CV), using a nanosized $Ca_3Co_4O_9$/Li half cell, at a scan rate of 0.1 $mV\,sec^{-1}$ (see Figure 2 a). The CV profiles of $Ca_3Co_4O_9$ in the first two cycles were almost identical to those of the Co_3O_4 nanostructures.[19] This proves that the CaO molecules in $Ca_3Co_4O_9$ do not react with lithium (CaO cannot be reduced to metallic Ca so easily because of its high bond strength).[20–22] Indeed, the CV profiles of CaO—measured on samples of similar mass and at the same voltage sweep rate—revealed that this species is electrochemically inactive (see Figure S2 of the Supporting Information). Therefore, the reduction peak at 0.62 V can be assigned to the reaction of lithium with $Ca_3Co_4O_9$ to form metallic Co, Li_2O, and the resultant CaO. This reduction peak shifts to a slightly higher voltage (namely, 0.88 V) in the subsequent cycles. In the oxidation scan of the CV profiles, two obvious oxidation peaks are observed at 1.36 and 1.92 V, which are attributed to the formation of α-CoO and the regeneration of Co_3O_4, respectively.[10] From the observations outlined above, the following reactions can be expected on the positive-electrode side of the $Ca_3Co_4O_9$/Li half cells:

$$Ca_3Co_4O_9 + 12\,Li \rightarrow 3\,CaO + 4\,Co + 6\,Li_2O \quad \text{(1st discharge)}$$

$$4\,Co + 6\,Li_2O \rightarrow {}^1/_3\,[4(Co_3O_4 + 8\,Li) + 2\,Li_2O] \quad \text{(1st charge)}$$

$${}^4/_3\,(Co_3O_4 + 8\,Li) \rightleftharpoons {}^4/_3\,(3\,Co + 4\,Li_2O) \quad \text{(subsequent cycles)}$$

Based on the first-discharge reaction, the calculated theoretical capacity of $Ca_3Co_4O_9$ would be 643.3 $mA\,h\,g^{-1}$ (that is, 12 Li species per formula unit). However, in the subsequent discharge–charge cycles a lower reversible capacity (of 571.8 $mA\,h\,g^{-1}$, which is equivalent to ≈10.7 Li species) is expected as a result of the subtraction of the inactive CaO contribution.

To provide a better understanding of the electrochemical performance of $Ca_3Co_4O_9$, voltage-specific capacity curves were obtained for the nanosized $Ca_3Co_4O_9$/Li half cell (see Figure 2 b). The cell was cycled at a rate of *C*/5 (here, *C* is defined as 12 Li ions per hour and per formula unit of $Ca_3Co_4O_9$). The first-specific-discharge capacity reaches a large value of ≈1230 $mA\,h\,g^{-1}$. Another feature of interest is that the first-discharge curve can be divided into three regions, as observed in the case of other metal oxides.[7,23,24] In region (1), the voltage drops rapidly to 1.5 V and then decreases gradually from 1.5 to 1.0 V, which corresponds to a discharge capacity of ≈50 $mA\,h\,g^{-1}$ (Figure 2 b, inset). We believe that this region of the first discharge is closely related to the insertion of a very small amount of Li ions into the $Ca_3Co_4O_9$ nanoplatelets before the subsequent destruction of the crystal structure. However, region (1) shows a different type of initial "extra" capacity in the other discharge curves (except for the first curve in the inset of Figure 2 b); this "extra" capacity was clearly observed in the early discharged stages of Co_3O_4 as a result of the formation of $Li_xCo_3O_4$ ($\approx Li_{1.47}Co_3O_4$).[7] For the second and third regions (that is, those between 1.0 and 0.01 V), the behavior of the discharge curve of $Ca_3Co_4O_9$ was similar to that of the Co_3O_4 nanoparticles. We believe that the second region (that is, the plateau at ≈0.9 V) and the third one (which reflects a continuous voltage drop down to 0.01 V) correspond to a conversion reaction that involves the decomposition of $Ca_3Co_4O_9$ into Co–CaO–Li_2O phases and the growth of a gel-like polymeric layer, respectively.[23] The first-specific-charge capacity of $Ca_3Co_4O_9$ is 761 $mA\,h\,g^{-1}$. The existence of an "extra" capacity, which is higher than the theoretical capacity in nanosized $Ca_3Co_4O_9$, can be attributed to the

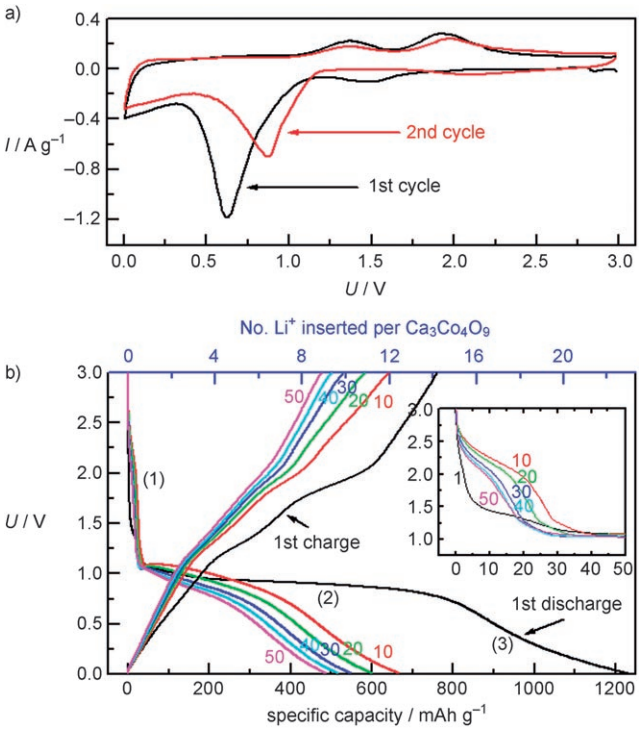

Figure 2. a) Typical cyclic voltammogram of the $Ca_3Co_4O_9$ powders at a scanning rate of 0.1 $mV\,s^{-1}$. b) Charging–discharging curves of the $Ca_3Co_4O_9$/Li half cells cycled between 3.00 and 0.01 V at a rate of *C*/5 (the $Ca_3Co_4O_9$ powders were calcined at 600 °C). The inset shows a magnified view of the initial discharge profiles for each cycle between 3–1 V.

 © 2007 Wiley-VCH Verlag GmbH & Co. KGaA, Weinheim

reversible formation of a Li-bearing solid–electrolyte interface.[6] The compound $Ca_2Co_2O_5$ was reported to exhibit a reversible capacity of 365–380 mA h g^{-1}, which is comparable to that of graphite (namely, ≈372 mA h g^{-1}).[20] However, we observed a reversible capacity of ≈500 mA h g^{-1} (even after 50 cycles) in $Ca_3Co_4O_9$, which is much higher than that of graphite-based negative electrodes.

For comparison, nanosized Co_3O_4 powders were also prepared by means of the citrate–gel method (see Figure S3 of the Supporting Information). The reversible capacity of these powders was high but faded rapidly after ten cycles, as shown in Figure 3. A fast capacity decay was also observed between

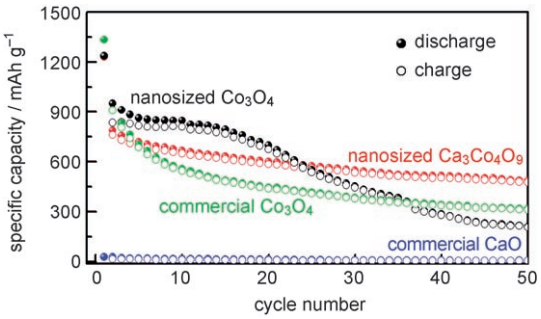

Figure 3. Variation of the discharge–charge specific capacity versus the cycle number for the nanosized $Ca_3Co_4O_9$ and Co_3O_4 powders calcined at 600 and 400 °C, respectively (the data obtained for commercial Co_3O_4 and CaO powders are also shown for comparison).

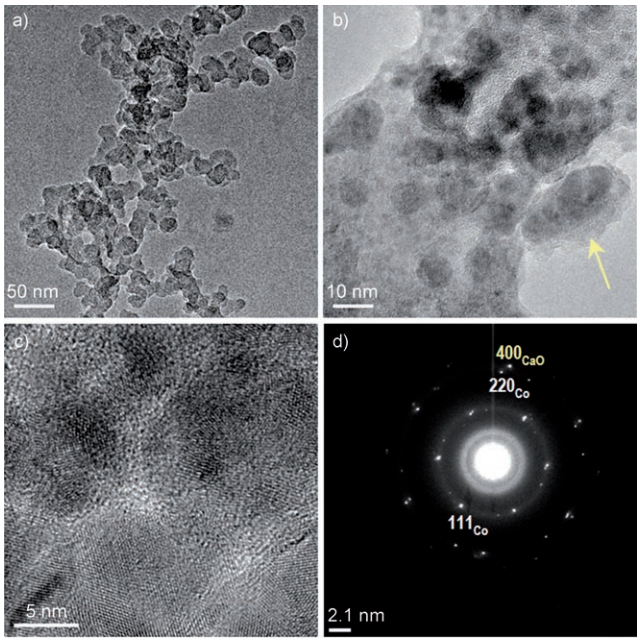

Figure 4. a) Low-magnification image of fully lithiated nanosized $Ca_3Co_4O_9$ powders (taken after five cycles). b, c) Magnified HRTEM images of (a). The lattice fringes of the nanocrystals inside the powder matrix are clearly shown in (c). The measured lattice spacings in the SAD pattern of (d) correspond to the (111) and (220) planes of Co and to the (400) plane of CaO.

the first (≈850 mA h g^{-1}) and the twentieth cycle (≈550 mA h g^{-1}) for other nanostructured Co_3O_4 materials, such as nanotubes or nanorods.[25] The capacity retention of the nanosized $Ca_3Co_4O_9$ particles was better than those of both the nanosized Co_3O_4 particles and the irregular, micro-sized commercial Co_3O_4 powder. The contribution of CaO to the lithium storage capacity was negligible, as expected.

To obtain a closer insight into the conversion reaction, we carried out HRTEM observations of the $Ca_3Co_4O_9$ powders in the discharged state; Figure 4a shows a bright-field image of such powders (at ≈0.01 V). Surprisingly, the $Ca_3Co_4O_9$ thin nanoplates were homogeneously pulverized into nanoparticles (with sizes of 30–50 nm). This behavior was also observed in the first-discharged and charged states. Furthermore, very little localized segregation of the nanocrystalline phases was detected, as shown in Figure 4b,c. We believe that the discharged nanoparticles have a complex nanocomposite structure, in which crystalline Co nanograins (with a diameter of less than 10 nm) are combined with pseudo-amorphous Li_2O and CaO; this structure is further confirmed by the selected-area (electron) diffraction (SAD) pattern shown in Figure 4d. The formation of a veil-like polymeric layer was also observed (as indicated by the arrow in Figure 4b). It was reported that the simple mixing of nanosized Co_3O_4 powders with conductive spherules cannot suppress the aggregation of the nanoparticles.[10] Here, CaO only acts as an inactive matrix. The advantages of this type of "spectator" matrix have been already reported for Sn- and transition-metal-based compounds.[20–22] Our results demonstrate that the formation of CaO after pulverization in the initial discharged state has beneficial effects on the electrochemical characteristics—especially on the reversible capacity retention. These effects result from the alleviation of the mechanical stress induced by the volume change of the active regions and from the prevention of the aggregation of the Co nanograins upon cycling.

Layered cobaltite ($Ca_3Co_4O_9$) exhibits an excellent electrical conductivity. Additionally, nanocomposite electrodes consisting of highly dispersed Co nanoclusters in an amorphous matrix are expected to retain their high internal electrical contact after conversion upon cycling. Indeed, the increase in cell polarization, which was observed for nanosized Co_3O_4 as a result of the formation of a solid–electrolyte interface (SEI) surrounding the active particles, was not observed in the case of nanosized $Ca_3Co_4O_9$—not even after 50 cycles, see the galvanostatic voltage–capacity curves in Figure 2b. Another good characteristic of nanosized $Ca_3Co_4O_9$ powders is their high-rate capability (see Figure 5): At Li insertion/extraction rates of 1*C*, 5*C*, and 10*C*, the nanosized $Ca_3Co_4O_9$ particles delivered specific capacities of 660, 320, and 190 mA h g^{-1}, respectively, thus maintaining an excellent coulombic efficiency of over 95% (that is, a high ratio of extractable-to-inserted Li). This high-rate capability results from the advantageous transport properties of the nanosized powders (such as shorter electron–Li-ion transport lengths and a higher electrode–electrolyte contact area) as well as from the electrochemically assembled (Li-driven) active/inactive nanocomposite structure, which suppresses undesirable electrode–electrolyte

 © 2007 Wiley-VCH Verlag GmbH & Co. KGaA, Weinheim

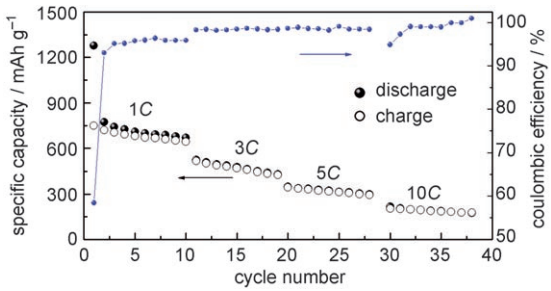

Figure 5. Cycling behavior and coulombic efficiency for the nanosized $Ca_3Co_4O_9$ particles cycled at different *C* rates.

processes (such as the formation of an SEI layer) and prevents the internal loss of electrical contact.[1]

In summary, we reported on a new layered electrode material—namely, nanosized $Ca_3Co_4O_9$—which shows a high and reversible specific capacity. The reaction entails a Li-driven conversion process, which results in the formation of an active/inactive nanocomposite electrode composed of highly dispersed Co nanoclusters embedded in a pseudo-amorphous Li_2O–CaO matrix. This nanocomposite electrode, which contains an inactive CaO matrix, was shown to improve the cycling performance and the rate capability. Additionally, since $Ca_3Co_4O_9$ can be successfully used as a *p*-type component in thermoelectric modules and as a negative electrode in Li-ion batteries, we expect that this new material will enable the fabrication of efficient energy-harvesting systems, which can recharge a Li-ion battery by using the power generated by the thermoelectric devices.[26]

Experimental Section

To prepare homogeneous nanosized $Ca_3Co_4O_9$ particles, polybasic chelates were formed using citric acid, $HOC(CH_2CO_2H)_2{\cdot}CO_2H$, with metallic ions.[27,28] Reagent-grade $Ca(NO_3)_2{\cdot}4H_2O$ and $Co(NO_3)_2{\cdot}6H_2O$ were weighed in specific proportions (to obtain the nominal composition of $Ca_3Co_4O_9$) and subsequently added to deionized water (1 L) and citric acid. In the resulting clear solution, the molar concentration of all metallic ions and the citric-acid-to-metal-ion molar ratio were controlled to be 0.327 M and 1.286:1, respectively. The solution was refluxed at 80 °C for 5 h (under stirring), followed by drying at 100 °C in a vacuum oven. This dehydrated solution gradually changed into a purple, rigid, glassy gel. The resultant gel was ignited in air at 400 °C (for 24 h) to produce an intermediate powder by combustion/oxidation, which was calcined to produce the final $Ca_3Co_4O_9$ nanosized powders at 600–700 °C in an O_2 atmosphere (to burn out the residual carbon). For the electrochemical evaluation of these powders, positive electrodes were prepared by mixing $Ca_3Co_4O_9$ (2–3 mg) with Super P carbon black (MMM Carbon, Brussels, Belgium) and the Kynar 2801 binder (PVdF-HFP) at a mass ratio of 67:20:13. The assembled Swagelok-type cells were galvanostatically cycled between 3.0 and 0.01 V by using a Toyo system automated tester (TOSCAT-3100, Toyo System Co., LTD., Fukushima, Japan).[19,29] The powders were characterized by means of XRD (M18XHF, Macscience Instruments, Japan) and HRTEM (JEM-3000F, JEOL, Japan).

Received: April 13, 2007
Revised: May 21, 2007
Published online: August 2, 2007

Keywords: composites · electrochemistry · lithium · nanomaterials · oxides

[1] A. S. Aricò, P. Bruce, B. Scrosati, J. M. Tarascon, W. V. Schalkwijk, *Nat. Mater.* **2005**, *4*, 366.
[2] M. Broussely, G. Archdale, *J. Power Sources* **2004**, *136*, 386.
[3] Y. Wang, J. Y. Lee, *Angew. Chem.* **2006**, *118*, 7197; *Angew. Chem. Int. Ed.* **2006**, *45*, 7039.
[4] S. H. Ng, J. Wang, D. Wexler, K. Konstantinov, Z. P. Guo, H. K. Liu, *Angew. Chem.* **2006**, *118*, 7050; *Angew. Chem. Int. Ed.* **2006**, *45*, 6896.
[5] E. Kim, D. Son, T. G. Kim, J. Cho, B. Park, K. S. Ryu, S. H. Chang, *Angew. Chem.* **2004**, *116*, 6113; *Angew. Chem. Int. Ed.* **2004**, *43*, 5987.
[6] P. Poizot, S. Laruelle, S. Grugeon, L. Dupont, J. M. Tarascon, *Nature* **2000**, *407*, 496.
[7] D. Larcher, G. Sudant, J. B. Leriche, Y. Chabre, J. M. Tarascon, *J. Electrochem. Soc.* **2002**, *149*, A234.
[8] G. X. Wang, Y. Chen, K. Kostantinov, J. Yao, J. H. Ahn, H. K. Liu, S. X. Dou, *J. Alloys Compd.* **2002**, *340*, L5.
[9] S. A. Needham, G. X. Wang, K. Konstantinov, Y. Tournayre, Z. Lao, H. K. Liu, *Electrochem. Solid-State Lett.* **2006**, *9*, A315.
[10] R. Yang, Z. Wang, J. Liu, L. Chen, *Electrochem. Solid-State Lett.* **2004**, *7*, A496.
[11] O. Mao, R. L. Turner, I. A. Courtney, B. D. Fredericksen, M. I. Buckett, L. J. Krause, J. R. Dahn, *Electrochem. Solid-State Lett.* **1999**, *2*, 3.
[12] S. Li, R. Funahashi, I. Matsubara, K. Ueno, H. Yamada, *J. Mater. Chem.* **1999**, *9*, 1659.
[13] I. Matsubara, R. Funahashi, T. Takeuchi, S. Sodeoka, T. Shimizu, K. Ueno, *Appl. Phys. Lett.* **2001**, *78*, 3627.
[14] Y. Masuda, D. Nagahama, H. Itahara, T. Tani, W. S. Seo, K. Koumoto, *J. Mater. Chem.* **2003**, *13*, 1094.
[15] H. Itahara, W. S. Seo, S. Lee, H. Nozaki, T. Tani, K. Koumoto, *J. Am. Chem. Soc.* **2005**, *127*, 6367.
[16] A. C. Masset, C. Michel, A. Maignan, M. Hervieu, O. Toulemonde, F. Studer, B. Raveau, J. Hejtmanek, *Phys. Rev. B* **2000**, *62*, 166.
[17] Y. Liu, Y. Lin, Z. Shi, C. W. Nan, Z. Shen, *J. Am. Ceram. Soc.* **2005**, *88*, 1337.
[18] S. Sakamoto, M. Yoshinaka, K. Hirota, O. Yamaguchi, *J. Am. Ceram. Soc.* **1997**, *80*, 267.
[19] K. T. Nam, D. W. Kim, P. J. Yoo, C. Y. Chiang, N. Meethong, P. T. Hammond, Y. M. Chiang, A. M. Belcher, *Science* **2006**, *312*, 885.
[20] N. Sharma, K. M. Shaju, G. V. S. Rao, B. V. R. Chowdari, *Electrochim. Acta* **2004**, *49*, 1035.
[21] N. Sharma, K. M. Shaju, G. V. S. Rao, B. V. R. Chowdari, *Electrochem. Commun.* **2002**, *4*, 947.
[22] N. Sharma, K. M. Shaju, G. V. S. Rao, B. V. R. Chowdari, Z. L. Dong, T. J. White, *Chem. Mater.* **2004**, *16*, 504.
[23] S. Grugeon, S. Laruelle, L. Dupont, J. M. Tarascon, *Solid State Sci.* **2003**, *5*, 895.
[24] Y. S. Hu, L. Kienle, Y. G. Guo, J. Maier, *Adv. Mater.* **2006**, *18*, 1421.
[25] W. Y. Li, L. N. Xu, J. Chen, *Adv. Funct. Mater.* **2005**, *15*, 851.
[26] R. Funahashi, M. Mikami, T. Mihara, S. Urata, N. Ando, *J. Appl. Phys.* **2006**, *99*, 066117.
[27] M. P. Pechini, U. S. Patent No. 3,330,697, **1967**.
[28] D. Segal, *J. Mater. Chem.* **1997**, *7*, 1297.
[29] D. Guyomard, J. M. Tarascon, *J. Electrochem. Soc.* **1993**, *140*, 3071.

 © 2007 Wiley-VCH Verlag GmbH & Co. KGaA, Weinheim